SOME ASPECTS OF WEATHER SYSTEMS DURING THE VENEZUELAN RAINY SEASON

by

MARTHA P. MATA

DEPARTMENT OF ATMOSPHERIC SCIENCE
COLORADO STATE UNIVERSITY
FORT COLLINS, COLORADO

SOME ASPECTS OF WEATHER SYSTEMS DURING THE VENEZUELA RAINY SEASON

by

Martha P. Mata

A Report prepared on the Venezuela Meteorological and Hydrological Experiment of 1969 under a research contract between the U.S. Department of Defense and Colorado State University

May 1972

ABSTRACT

SOME ASPECTS OF WEATHER SYSTEMS DURING
THE VENEZUELA RAINY SEASON

Over Venezuela, as in the tropics in general, synoptic weather systems on daily charts may be either dry or they may be heavy precipitation producers. Vertical advection of vorticity cannot be used to serve as a criterion to delineate regions of ascent as in higher latitudes. Hence other computational approaches are tried out, designed to identify those synoptic systems that produce precipitation from similar appearing ones that do not.

Active tropical weather disturbances should have divergence at 200 mb and convergence in the low troposphere. But calculations of kinematic divergence during the period July-September 1969 for eastern Venezuela during Project VIMHEX I did not show a useful correlation perhaps due to the problems in determinating divergences kinematically. Calculations using the vorticity equation also did not give the expected convergence-divergence problem so that, given present extent and quality of the synoptic upper-air network over the Caribbean and northern South America, specification cannot be expected from the wind data.

Next, heat balance calculations were performed, especially during periods of tropospheric cold air advection at the approach of upper troughs toward eastern Venezuela. It is shown that radiational heat loss is a major factor in such calculations. Bulk methods to calculate vertical motion in clear areas and in synoptic-scale cloudy areas are developed. Results are presented for both the VIMHEX operational area where daily rainfall data were available, and for the oceanic area of

the northeastern Caribbean. Again, the calculations failed to show obvious differences between dry and moist synoptic systems; however it is hoped that enough of an advance has been made so that, using the present basis, further results can be obtained during the 1972 VIMHEX II operation.

ACKNOWLEDGEMENT

This research was performed while the author was a graduate student at Colorado State University, under a research contract between the Office of Naval Research and Colorado State University. Project VIMHEX I, directed by Professor Herbert Riehl, was a joint enterprise of Colorado State University and agencies of the Venezuelan Government, especially the Meteorological Service of the Venezuelan Air Force. The author wishes to thank Professor Riehl for his support and encouragement during the study and suggestions on the preparations of this manuscript. Thanks are also extended to Mrs. Pat Johnson and Miss Karla Garretson for their assistance with preparation and typing.

INTRODUCTION AND OBJECTIVES

One of the major meteorological problems of the present time is the prediction of tropical synoptic weather systems and their associated precipitation. During the years since 1950 forecasting in middle and higher latitudes by qualitive models and experience has been replaced, at least as far as the large-scale pressure and windfield is concerned, by quantitative techniques. In the tropics the physics of weather disturbances as yet is not sufficiently well known for quantitative prediction methods to be put on a routine basis. A large amount of interest, therefore, centers on the development of adequate prediction techniques.

The main problem confronting the tropical forecaster is that synoptic systems do not draw upon potential energy stored in a broad belt with temperature concentration where the potential energy may be readily released. Rather, much of the energy infusion in the tropics occurs via the condensation-precipitation process. However, as already pointed out by Riehl (1948), there is a serious difficulty in tracing the energy cycle because tropical rain areas often are cold-cored and not warm-cored as would be required for a direct utilization of condensation heat to generate kinetic energy. This problem survives to the present day.

The objective of this research is to make a further examination of tropical synoptic systems from the forecasting viewpoint. For this purpose synoptic charts of the troposphere, ESSA, NIMBUS and ATS III satellite photos, as well as special observations taken during Project VIMHEX I in eastern Venezuela, were utilized for the period July-September 1969. Project VIMHEX (Venezuela International Meteorological

and Hydrological Experiment) had its headquarters at Anaco (Fig. 1), where daily map analyses at the surface, at 850 and 200 mb were carried out. These maps were later augmented using charts furnished by the National Hurricane Center, Miami. Of the special project data our present interest centers mainly in the rain gauge observations. A daily rainfall average was computed for the stations inside the circular area with radius of 80 km "seen" by a radar installation at Anaco which was monitoring the mesoscale cloud systems passing through the region (Fig. 2).

Given the foregoing three sources of information--synoptic charts, satellite photos and local rain index--the problem is to specify where and when precipitation will occur and to relate such precipitation to the further evolution of the weather patterns.

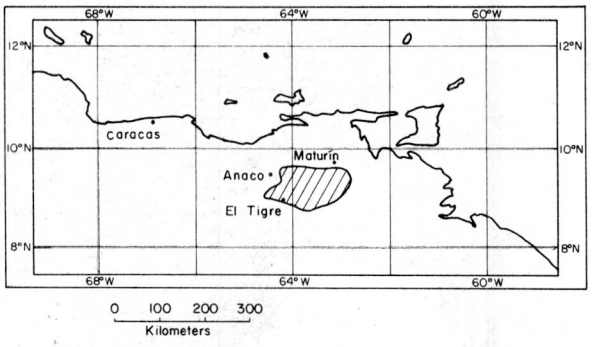

Figure 1. Location of experimental area in 1969. Anaco was headquarters. Shading indicates watersheds for hydrologic computations.

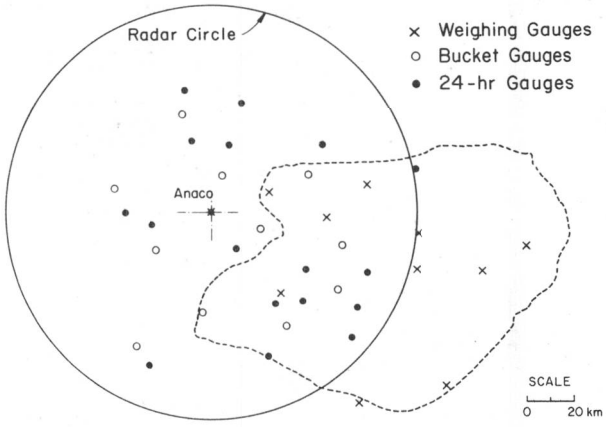

Figure 2. Rain gauges in area seen by radar around Anaco.

CLASSIFICATION OF SYNOPTIC SITUATION

Vertical Vorticity Gradient: In principle, one desirable criterion would be to stratify all days of a sample directly according to whether a given region has a cold, warm or an indifferent thermal field with respect to the surroundings. Such a classification was attempted for northeastern Venezuela; it had to be abandoned on account of lack of reliability of thermal fields. However, the windshear above the layer of cumulus convection is a good indicator of the temperature field even at latitude 10^{o}, i.e. the geostrophic thermal shear approximates the temperature field of the troposphere fairly well. Hence, a vorticity classification was next devised, based on the difference in relative vorticity about the vertical axis (ζ) between 850 and 200 mb.

Because of predominant lower easterlies the vertical vorticity gradient was determined mostly by the circulations at 200 mb. On many days the 200 mb vorticity field could be estimated readily; on other days with a weak or rapidly changing winds much uncertainty remains. At 850 mb problems of classification arose only during presence of equatorial west winds. On such days a narrow zone of high vorticity should exist along the boundary between these westerlies and the trades farther north. However, the windfield often was too weak and the definition of the equatorial shear zone not clear enough to place the high vorticity area accurately. Further, satellite cloud photos and low-level shear zone did not appear correlated, thus no help was obtained from satellite information.

With these limitations in mind, the vertical vorticity difference (200 minus 850 mb) was divided into three classes:

Group I: $\Delta\zeta > 0.5 \times 10^{-5}$ sec^{-1} (mostly cold trough)

Group II: $\Delta\zeta \pm 0.5 \times 10^{-5}$ sec^{-1} (indifferent)

Group III: $\Delta\zeta < -0.5 \times 10^{-5}$ sec^{-1} (mostly warm ridge)

A difference of 0.5×10^{-5} sec^{-1} corresponds to 20 percent of the Coriolis parameter at latitude 10^{o}. Choice of larger class intervals, with more certainty of accuracy of classification, was not feasible. For instance, with a limit of 1.0×10^{-5} sec^{-1} for the vorticity difference, most cases would have been classified as "indifferent".

Rainfall Index: The daily rainfall index within the radar circle served to classify days as "dry" or "wet" and to define "rain episodes" (see Riehl, et al, 1972). A day is taken as "wet" if it exceeds the average daily precipitation of the study period which is 4.4 mm. The days with precipitation greater than the mean accounted for 75 percent of all precipitation; there were 32 such days, or 35 percent of all days. A rainfall episode was defined as one or more days with precipitation exceeding the limit of 4.4 mm/day. There were 15 such episodes, ranging in duration from one to nine days.

Combined Classification: Given a synoptic and a rainfall classification for each day, a contingency table yielding a combined index may now be constructed (Table 1). From this table it is seen that the synoptic classification alone yields a reasonable frequency distribution. It is also evident that cold and warm cored systems may be either wet or dry, bringing out again the difficulty mentioned by Riehl (1948). Thus, from inspection of synoptic charts alone, one cannot locate rain areas in contrast to higher latitudes where most rain areas at least lie in an area with lower cyclonic vorticity changing to upper anticyclonic vorticity. If a parameterization of convective processes relative to

synoptic envelopes is desired, stratification according to vertical vorticity difference or implied thermal field will not serve in general, an outcome of the statistic that was anticipated and which is once again verified by Table 1.

TABLE 1

Synoptic Classification of Days: Groups as defined in Text

	Group		
Days	I	II	III
Dry	17	16	15
Wet	14	1	22
Total	31	17	37

TOTAL NUMBER OF DAYS - 85

Still another question may be asked, namely whether warm upper ridges deliver much more rain than cold troughs. As Table 2 indicates, this is not the case, at least to any significant degree; nor does the cloud population show distinct differences between Synoptic Groups I and III (Riehl, et al, 1972). Thus, the quest for factors relating synoptic structure and rain areas must develop along new lines. In order to limit the problem to synoptically comparable developments, seven three-day sequences were selected during which a transformation from Group III to Group I occurred, i.e. an upper ridge was replaced by an upper trough in eastern Venezuela. Table 3 gives the dates selected; three of the cases were "dry" and four were "wet" on the central day, so that Table 3 gives both a synoptic and a rain productiveness stratification.

TABLE 2

Daily Precipitation (mm) in Radar Circle
Averaged according to Synoptic Groups

	Group		
	I	II	III
Wet	7.4	-	9.9
Dry	1.6	1.1	1.4
Dry, excluding Zero Rain Index Days	2.3	2.2	1.7

TABLE 3

Days Chosen for this Study, Including Precipitation and Classification

Date	Days	RR (cm/d)	Synoptic Classification	w = wet day d = dry day
RAINY GROUPS				
7/9/69	D-1	0.5	III	w
7/10/69	D	1.5	III	w
7/11/69	D+1	1.7	I	w
8/7/69	D-1	0.1	III	d
8/8/69	D	2.0	III	w
8/9/69	D+1	0	I	d
8/11/69	D-1	1.9	III	w
8/12/69	D	2.8	III	w
8/13/69	D+1	0.6	I	w
8/22/69	D-1	0.3	II	d
8/23/69	D	1.4	III	w
8/24/69	D+1	0.8	I	w
DRY GROUPS				
7/31/69	D-1	0.1	II	d
8/1/69	D	0.3	III	d
8/2/69	D+1	0.3	I	d
8/19/69	D-1	0.5	III	w
8/20/69	D	0.2	III	d
8/21/69	D+1	0.1	I	d
9/8/69	D-1	1.2	III	w
9/9/69	D	0	III	d
9/10/69	D+1	0.6	I	w

DIVERGENCE CALCULATIONS

The first attempt made concerned the divergence field. If this field and its attendant large-scale vertical motion field were known, a relation to precipitation might well be established.

Kinematic Calculation: Initially, divergence was calculated from rawinsonde data with the Bellamy (1949) method. At 200 mb, we should find positive divergence associated with convective areas, since the outflow from cumulonimbi tends to be concentrated around 200 mb where outflow velocities from the topics poleward are greatest and where the high-tropospheric synoptic systems of low latitudes have their greatest intensity. Hence, 200-mb divergence calculations were made for each day listed in Table 3 at 1200Z; stations used were Curacao, Anaco and Trinidad (Fig. 3) which yield only a flat triangle with the Anaco radar circle at one edge. Table 4 gives the results. Order of magnitude of divergence is 10^{-6} - 10^{-5} sec^{-1}, which is the expected magnitude for areas of the size considered. Correlation with radar circle precipitation is not at all positive as should be the case; it may be mentioned that the precipitation usually occurred within 8-12 hours from map time. While it is true that the triangle does not enclose the radar circle well, and the latter's area is only a small fraction of the triangle, nevertheless Anaco precipitation on most days is rather well correlated with that of larger areas around it and a better relation to the 200-mb divergence should have been found.

The results agree with various unpublished studies by Riehl and by the National Hurricane Center and not, unfortunately, with the fine correlation found by Reed (1971) and others for Pacific disturbances. Various numerical modelers of recent years have tried to smooth and

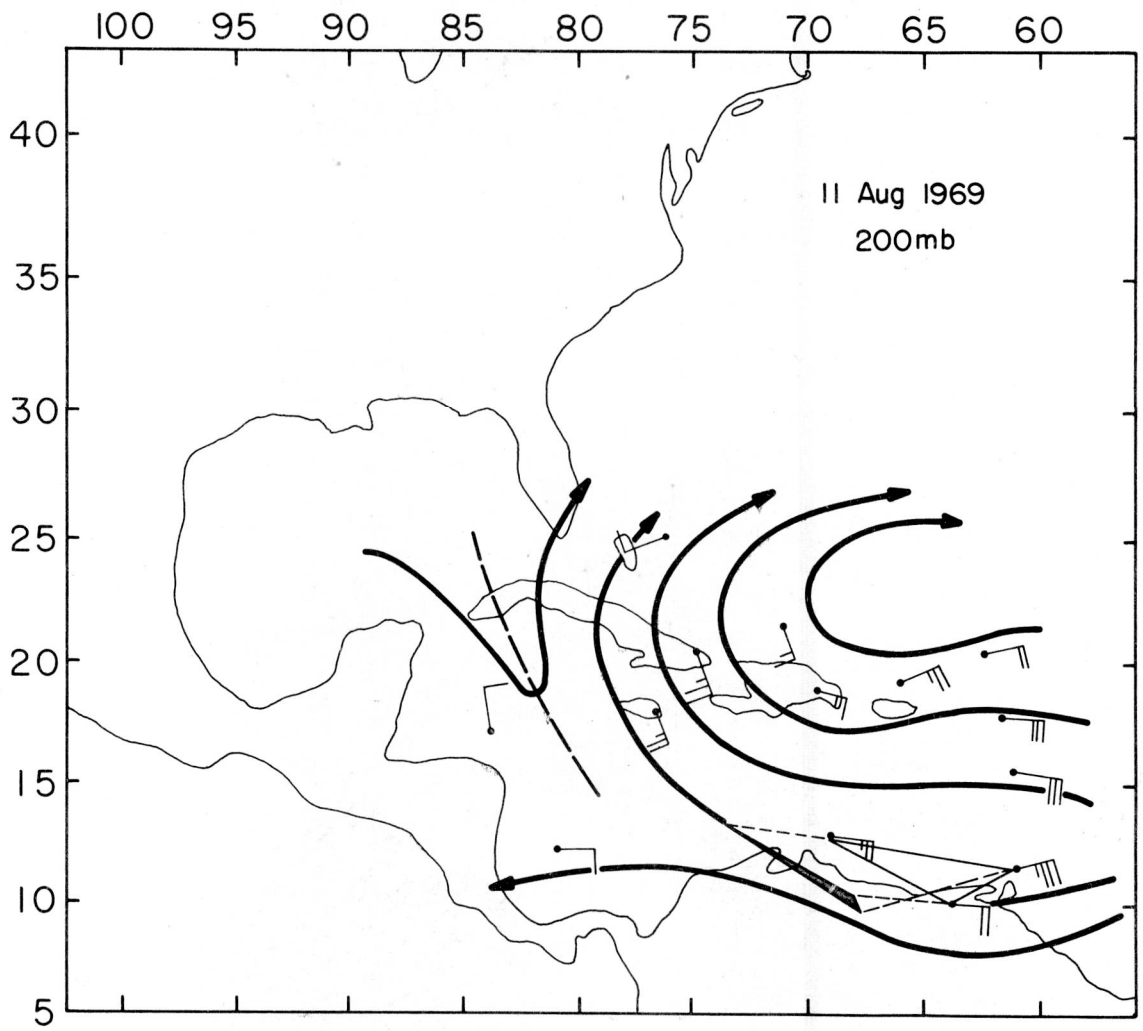

Figure 3. 200-mb winds over Caribbean, 11 August 1969, 1200Z, and illustration of kinematic method used for computation of divergence in the triangle Curacao-Anaco-Trinidad.

control, i.e. "massage", vertical motion fields by resorting to large-sample treatments, mass continuity restraints and other devices. If our calculations had been somewhat better, we might have been encouraged to follow along some of these lines. But it is clear that the basic data must provide some real encouragement for refinement, and this is clearly not the case here.

Using the same type of calculation for a low level triangle (3,000 and 5,000 ft), again no correlation with precipitation of the area was found. This low level triangle had in one corner Trinidad and in the other corner Anaco and Tumeremo; Maturin and Ciudad Bolivar were also included.

Vorticity Advection: A second attempt was made to determine the 200-mb divergence field using the vorticity equation. This should give some indication whether perhaps just the kinematic computation method is unreliable and whether a dynamical determination of divergence will give superior results.

The vorticity equation for large-scale flow in the free atmosphere on constant pressure surfaces,

$$\frac{d}{dt}(f + \zeta) = - (f + \zeta)\nabla \cdot V \qquad (1)$$

where f is the Coriolis parameter and $\nabla \cdot V$ horizontal divergence measured on constant pressure surfaces--essentially horizontal surfaces in the tropics. We assume that at 200 mb the vertical gradient of vorticity is near zero, since the synoptic systems attain their greatest intensity there, also that local changes with time are slow. It is not necessary to make this last assumption, since we do have the

time sequence of vorticities; it appears sufficient however to approximate

$$\frac{d}{dt}(f + \zeta) = V \frac{\partial}{\partial s}(f + \zeta), \qquad (2)$$

the horizontal vorticity advection along the streamlines where s is the axis along the wind direction (streamline) and V the horizontal wind. The relative vorticity $\xi = K_s V + \frac{\partial V}{\partial n}$ where K_s is curvature of the streamlines and n the coordinate perpendicular to s and the positive to its right. Only the first of these two terms could be reliably determined in eastern Venezuela; for a shear calculation at least one additional rawinsonde station to the south of Anaco would have been required. We shall approximate $\zeta = K_s V$. Further, $\partial f/\partial s = \beta \sin\alpha$. Here β is the variation of the Coriolis parameter with latitude, also constant at 2×10^{-13} cm^{-1} sec^{-1} in the topics; α is the angle between a latitude circle and the streamline, positive for quadrant between W and N, negative for quadrant between S and W. Selecting now two points (1) downstream and (2) an equal upstream from Anaco along a streamline passing through the station, equation 1 may be written with the foregoing transformation as

$$-\nabla \cdot V = \frac{V}{f+\xi}\left(\beta \sin\alpha + \frac{(VK_s)_2 + (VK_s)_1}{\Delta s}\right) \qquad (3)$$

where Δs is the distance between points 1 and 2, generally chosen on the order of 1,000 km. In addition to equation 3 we tried the reduced form

$$-\nabla \cdot V = V \frac{\beta}{f} \sin\alpha = V \sin\alpha \times 10^{-8} \text{ sec}^{-1}, \qquad (4)$$

since at latitude 10 we have $f = 2 \times 10^{-5}$ sec^{-1} approximately, so that $\beta/f = 10^{-8}$ cm^{-1}. The large value of this ratio near the equator is the reason for considering equation 4 as a possibly valid expression. Tables 5 and 6 show the divergence computation using equations 3 and 4. These tables are just as disappointing as Table 4. There is a small margin in favor of equation 4 (Table 6); however results are not good enough to warrent computing a correlation coefficient.

This phase of the investigation herewith has not been successful. The lack of success is not necessarily ascribed to the physical principles tested but to lack of observations for making adequate tests. Better results should be obtained if the synoptic network is expanded, including satellite-derived wind, so that the field of velocity and of velocity gradients is adequately described.

TABLE 4

Divergence Calculated by the Kinematic Method

Group: III → I
Level: 200 mb

Days:	(D - 1)			(D)*				(D + 1)			
1969 Date	$\nabla \cdot V \times 10^{-5}$ (sec^{-1})	RR (cm/d)	Class	1969 Date	$\nabla \cdot V \times 10^{-5}$ (sec^{-1})	RR (cm/d)	Class	1969 Date	$\nabla \cdot V \times 10^{-5}$ (sec^{-1})	RR (cm/d)	Class
RAINY GROUPS											
7/9	-0.9	5	III, w	7/10	-0.6	15	III, w	7/11	+2.5	17	III, w
8/7	+0.9	1	III, d	8/8	-2.6	20	III, w	8/9	-2.9	0	I, d
8/11	-3.6	19	III, w	8/12	-0.2	28	III, w	8/13	+2.1	6	I, w
8/22	-3.1	3	II, d	8/23	-0.1	14	III, w	8/24	-1.0	8	I, w
DRY GROUPS											
7/31	+0.8	1	II, d	8/1	+0.6	3	III, d	8/2	0	3	I, d
8/19	0	5	III, w	8/20	+0.4	2	III, d	8/21	-1.5	1	I, d
9/8	+0.4	12	III, w	9/9	0	0	III, d	9/10	-1.6	6	I, w

*D denotes central day of sequency.

TABLE 5

Divergence Calculated by the Relative Vorticity Equation $\nabla \cdot V = \frac{V}{f+\xi}\left(\beta \sin\alpha + \frac{(K_s V)_2 - (K_s V)_1}{\Delta s}\right)$

Group: III → I
Level: 200 mb
Station: Anaco

Days:	(D - 1)			(D)*			(D + 1)		
1969 Date	$\nabla \cdot V \times 10^{-5}$ (sec^{-1})	RR (cm/d)	Class	1969 Date	$\nabla \cdot V \times 10^{-5}$ (sec^{-1})	RR (cm/d)	Class	1969 Date	$\nabla \cdot V \times 10^{-5}$ (sec^{-1})	RR (cm/d)	Class
RAINY GROUPS											
7/9	-0.9	5	III, w	7/10	+0.9	15	III, w	7/11	+1.7	17	III, w
8/7	+0.6	1	III, d	8/8	-1.2	20	III, w	8/9	+0.5	0	I, d
8/11	-2.2	19	III, w	8/12	-14.0	28	III, w	8/13	-2.2	6	I, w
8/22	+0.3	3	II, d	8/23	+0.5	14	III, w	8/24	-2.8	8	I, w
DRY GROUPS											
7/31	-0.8	1	II, d	8/1	-	3	III, d	8/2	+0.3	3	I, d
8/19	+5.5	5	III, w	8/20	+0.7	2	III, d	8/12	+0.8	1	I, d
9/8	+0.4	12	III, w	9/9	-0.6	0	III, d	9/10	+1.0	6	I, w

*D denotes central day of sequence.

TABLE 6

Divergence Calculated by the Reduced Vorticity Equation $\nabla \cdot V = V \sin\alpha \times 10^{-8}$ (sec^{-1})

Group: III → I
Level: 200 mb
Station: Anaco

Days:	(D - 1)			(D)*			(D + 1)			
1969 Date	$\nabla \cdot V \times 10^{-5}$ (sec^{-1})	RR (cm/d)	Class	1969 Date	$\nabla \cdot V \times 10^{-5}$ (sec^{-1})	RR (cm/d)	Class	1969 Date	$\nabla \cdot V \times 10^{-5}$ (sec^{-1})	RR (cm/d)	Class
RAINY GROUPS											
7/9	-1.2	5	III, w	7/10	+1.5	15	III, w	7/11	+0.8	17	III, w
8/7	+0.9	1	III, d	8/8	+0.3	20	III, w	8/9	+0.5	0	I, d
8/11	-1.1	19	III, w	8/12	+1.0	28	III, w	8/13	+1.4	6	I, w
8/22	+1.0	3	II, d	8/23	+0.6	14	III, w	8/24	-0.3	8	I, w
DRY GROUPS											
7/31	-0.6	1	II, d	8/1	+0.6	3	III, d	8/2	+0.1	3	I, d
8/19	+1.3	5	III, w	8/20	+0.7	2	III, d	8/21	+0.7	1	I, d
9/8	-0.1	12	III, w	9/9	-0.2	0	III, d	9/10	-1.0	6	I, w

*D denotes central day of sequence.

ENERGY BALANCE COMPUTATIONS

The synoptic sequence chosen for analysis--upper ridge being replaced by upper trough--generally features cold air advection into north-eastern Venezuela and also counterclockwise turning of wind with height. The geostrophic shear gives a fair approximation of the tropospheric temperature field and, together with the mean tropospheric wind, a reasonable estimate of the thermal advection. By examining the periods of such cold air advection more closely, it may be possible to make some deductions about the vertical motions present and also on the energy balance of the atmosphere during moist and dry episodes of this synoptic transformation. In order to gain a wider view, analysis for the whole central and eastern Carribean was carried out; however, the principal calculations were limited to northeastern Venezuela where we have daily measured rainfall value in the radar circle area.

Thermodynamic Considerations: The local rate of temperature change $\partial T/\partial t$ is related to the individual change through the well known Eulerian expansion

$$dT/dt = \partial T/\partial t + V\cdot\nabla T + w\,\frac{\partial T}{\partial Z} \quad . \tag{5}$$

Here the second term represents horizontal and the last term vertical advection. In middle latitudes a model stating that $\partial T/\partial t + V\cdot\nabla T = 0$ has been found to be valid, or nearly so, in many types of weather patterns, especially the long waves in the westerlies. Sources and sinks of thermal energy must be small relative to advection for this relation to hold; indeed, temperature changes in actively moving upper troughs and fronts have the magnitude of 10C/day which is an order of

magnitude larger than radiation cooling. In the tropics, the magnitude of advection decreases to 1C/day or even less, so that energy sources and sinks may never be omitted and the very simple formula above is not applicable even for 24-hour periods.

We must consider the first law of thermodynamics

$$\frac{dh}{dt} = c_p \frac{dT}{dt} - \frac{1}{\rho} \frac{dp}{dt} \tag{6}$$

where h is energy added to the system, c_p specific heat of air at constant pressure, ρ density and p pressure. The last term, through well known transformations, may be written as $1/\rho \, dp/dt = -gw$, where g is acceleration of gravity and w vertical motion. It is assumed that local changes of pressure and cross-isobar flow are small compared to the vertical motion of mass through the pressure field, and that the atmosphere is in quasihydrostatic equilibrium. The last assumption causes no problem, since we are not concerned with the vertical balance of forces inside cumulonimbi themselves, but with the balance over large areas. Then

$$\frac{dT}{dt} = \frac{1}{c_p} \frac{dh}{dt} - \frac{g}{c_p} w \tag{7}$$

where $\frac{g}{c_p} = - \frac{\partial T}{\partial z})_a$, the dry-adiabatic lapse rate. Combining equations 5 and 7 and solving for the vertical motion,

$$w = - \frac{\frac{\partial T}{\partial t} + V \cdot \nabla T - \frac{1}{c_p} \frac{dh}{dt}}{g/c_p + \frac{\partial T}{\partial Z}} \tag{8}$$

In this equation the denominator may be taken as constant if we limit its meaning and application to the whole tropospheric cloud layer in

bulk which has a nearly invariant lapse rate of 0.67C/100m. Thus $g/c_p + \frac{\partial T}{\partial Z} = 3.3 \times 10^{-3}$ C/meter. The energy source term for the bulk of the troposphere $dh/dt = R + LP$, where R is the net radiation cooling, and L latent heat of condensation taken constant at 600 cal/gm and P precipitation depth.

From most recent satellite estimates[1] $R = 1.2$C/day for clear areas and 1.3C/day in cloudy areas, where, however, the actual cooling rate may be variable depending on presence or absence of cirrus overcasts at low temperatures. It was decided to use $R = -1.2$C in both clear and cloudy areas over sea. Over land where sensible heat transfer from the ground contributes almost half of the energy transfer into the atmosphere, the radiation estimate was cut by a factor of two since we are interested in the cloud layer alone and the net radiation to space includes also the subcloud layer[2]. Even after such reduction, the radiation term is as large as $\frac{\partial T}{\partial t} + V \cdot \nabla T$ on the right side of equation 8 in clear and cloudy areas.

For days without precipitation equation 8 becomes

$$\hat{w} = - \frac{\frac{\partial \hat{T}}{\partial t} + \widehat{V \cdot \nabla T} - R}{3.3 \times 10^{-3}} \text{ (m/day)}. \qquad (9)$$

where $\hat{}$ denotes vertical averaging. Table 7 gives vertical velocities without and with radiation; the large influence of radiation cooling at small $\frac{\partial T}{\partial t} + V \cdot \nabla T$ is readily seen. In the Caribbean summer atmosphere the computed vertical motion was always descending.

---

[1] Kindly supplied by Professor Stephen K. Cox, Atmospheric Science Department, Colorado State University.

[2] As suggested by Professor Alan Betts.

The vertical motion in equation 9 is generally applicable to a large area such as a square with side of several degrees latitude. On days with small but measurable precipitation, little error probably is incurred if the right side of equation 9 is merely reduced by the amount of precipitation. One can compute the amount of precipitation (P') needed to reduce $\hat{w}$ to zero. From the quantity P' - p, the precipitation deficit, the residual vertical motion $\hat{w}$ required for balance of equation 9 may be computed. Table 8 gives the relation.

On days with heavy precipitation the approach taken so far must be modified. From equations 8 and 9 only area-averaged vertical mean motions for the troposphere are computed, whereas it is well known that vertical mass transfer mainly occurs within clouds and that with updrafts, downdrafts and lateral entrainment present, the correct description of the mesoscale processes becomes very complex. These details have been the subject of many investigations of the last decade. It is not the intention here to become involved in this difficult subject but rather to define a bulk computational procedure for large precipitation areas. We accomplish this by setting

$$P = P' + P'', \tag{10}$$

where P' is the precipitation required to balance the right side of equation 9, as already specified, and P'' is the precipitation excess of P over P'. Then

$$L/c_p \, P' = - \left(\frac{\partial \hat{T}}{\partial t} + V \cdot \nabla T - R\right). \tag{11}$$

Table 9 shows the daily precipitation amounts required to balance equation 11. At -1.2C/day, the assumed radiation value, the corresponding

TABLE 7

Descending Vertical Velocities for Totally Dry Days as Calculated from Equations 8 and 9

$\frac{\partial T}{\partial t} + V \cdot \nabla T$ (^{o}/d)	W(m/d)	$\frac{\partial T}{\partial t} + V \cdot \nabla T + 1.2$ (^{o}/d)	W(m/d)
+2.0	-600	+3.2	-970
+1.5	-450	+2.7	-820
+1.0	-300	+2.2	-670
+0.5	-150	+1.7	-520
0	0	+1.2	-360
-0.5	+150	+0.7	-210
-1.0	+300	+0.2	- 60
-1.5	+450	-0.3	+ 90
-2.0	+600	-0.8	+240

TABLE 8

Deficit of Precipitation and Descending Vertical Velocity

RR (cm/d)	$w\downarrow$ (m/d)
0.1	-110
0.2	-220
0.3	-330
0.4	-440
0.5	-550

TABLE 9

Precipitation Calculated from Equation 11

$(\frac{\partial T}{\partial t} + V\cdot\nabla T - R)$ (^{o}C/d)	RR (cm/d)
0.7	0.21
0.8	0.24
0.9	0.27
1.0	0.30
1.1	0.33
1.2	0.36
1.3	0.39
1.4	0.42
1.5	0.45
1.6	0.48
1.7	0.51
1.8	0.54
1.9	0.57
2.0	0.60

precipitation is no less than 0.36 cm/day which is not far from the average daily precipitation of the whole equatorial trough zone and also the seasonal precipitation received in 1969 in northeastern Venezuela. It is seen that inclusion of sensible heat transfer from the ground and reduction of the net radiation to -0.6C/day makes a large difference.

The vertical motion corresponding to P" may be determined as follows if we assume this vertical motion to occur entirely within clouds and omit any involved updraft-downdraft model and also re-evaporation of part of the "condensate" as labelled by Rasmussen,

et al (1969)[1]. As noted by Riehl et al (1972) very little difference in moisture content of the atmosphere has been observed in northeastern Venezuela between dry and moist days; the advective fields also appear weak in contrast even to the Antilles, some 10 degrees latitude farther north. For Venezuela we may write with little approximation that $dq/dt = w\, \partial q/\partial z$, where q is specific humidity; it may be noted that the inclusion of $\partial q/\partial t + V\cdot\nabla q$ would pose no computational obstacle where this quantity has the same magnitude as the vertical transport term. With the foregoing approximation

$$P = -\int w \frac{\partial q}{\partial z} \frac{\delta P}{g} \quad . \tag{12}$$

Now $\partial q/\partial z = -q_o/\Delta z$, where q_o is specific humidity at cloud base and Δz the tropospheric thickness considered, i.e. 11 km. In this formulation upper outflow of water vapor has been neglected as insignificant; q_o may represent the average specific humidity of the subcloud layer. Also $\frac{\Delta P}{g} = -\hat{\rho}\Delta z$, so that

$$P = \hat{w}\, \hat{\rho} q_o$$

and

$$\hat{w}'' = P''/\hat{\rho} q_o, \tag{13}$$

where $\hat{w}''$ is now the in-cloud vertical velocity corresponding to the excess precipitation P''. For example, if we use $q_o = 15$ g/kg, $\hat{\rho} = 10^{-3}$ g/cm^3 and $P'' = 1$ cm/day, $\hat{w}'' = +700$ m/day averaged over the

---

[1] It may not be amiss, however, to point out that here exists an excellent potentiality for further development of a more complete physical model of rain areas.

whole area considered. If precipitating clouds are confined to 10 percent of a synoptic disturbance area, as suggested by Riehl and Malkus (1958) and Riehl, et al (1972) then the continuing $\hat{w}''$ in the clouds in this area is 7,000 m/day, still not very large. Table 10 gives values in in-cloud vertical motion related to precipitation.

TABLE 10

Ascending Vertical Velocity Corresponding to Precipitation.
All ascent is in clouds but values are area-averaged

w (m/d)	RR (cm/d)
0	0
60	0.1
120	0.2
180	0.3
240	0.4
300	0.5
700	1.0
1000	1.5
1400	2.0
1700	2.5
2100	3.0

PROCEDURE OF EVALUATION

Map analysis will yield the quantity $\frac{\partial T}{\partial t} + V \cdot \nabla T$, if observations are sufficiently accurate. Satellite photos can be used to decide which portions of the eastern Caribbean-Venezuela area were dry or moist. Except for the radar circle in Venezuela only P' can be estimated. An interesting question was whether any negative values of P' would be obtained. In view of the strong radiation cooling this did not happen; however, if radiation was much smaller in some situations than here assumed, negative values would arise which must be interpreted to mean that an area-averaged vertical motion $\tilde{w}$ would actually exist in the clear areas.

As already indicated, vertical shear charts and also thickness charts for the layer 850-200 mb were analyzed during Project VIMHEX on every day. Whenever any definite synoptic disturbance was present, the two sets of lines usually corresponded very well and also showed up occasional poor thickness values (Fig. 4). Sample computations of thermal advection from thickness charts plus charts of the mean vector wind for the 850-200 mb layer (Fig. 5) compared well with charts generated by using the mean layer wind and geostrophic thermal gradient at each station. The latter procedure, being most convenient, was adopted for this study. The local change in mean temperature was determined from the time sequence of three daily charts by drawing time-height profiles. This would have been an easier task if 12-hourly maps had been available. Fig. 6 is an example of a chart giving the right hand side of equation 12 which can then be used to calculate P' or also $\hat{w}$ using equation 9 in cloudless areas. Figs. 7-12 show the maps and computations for the following two days of the 11-13 August

1969 case of westward displacement of an upper tropospheric trough from the Atlantic into the Caribbean.

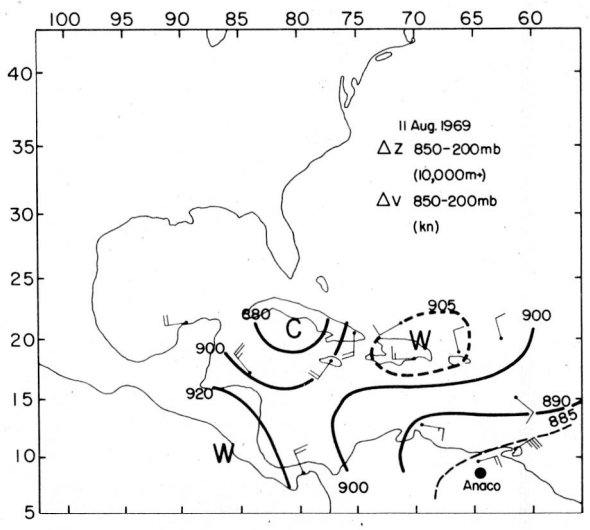

Figure 4. Wind shear vectors 850-200 mb (knots) and thickness between the 850 and 200-mb pressure surfaces (10,000 meters +) for 11 August 1969, 1200Z, illustrating relation between actual and geostrophic temperature fields.

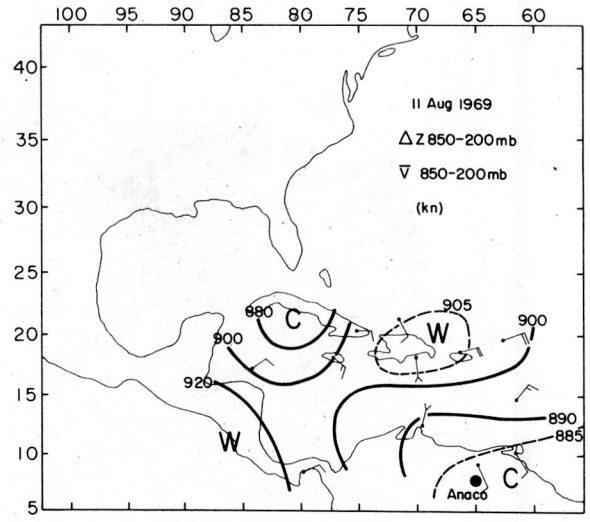

Figure 5. Thickness 850-200 mb for 11 August 1969 repeated from Figure 4 and mean vector wind 850-200 mb (knots) showing regions of warm and cold advection.

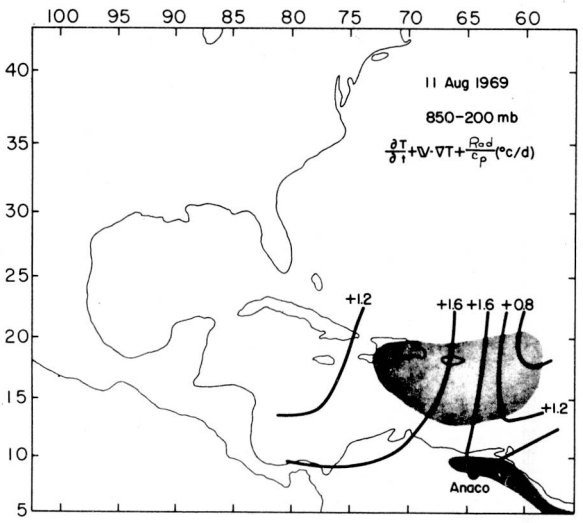

Figure 6. Field distribution of $\frac{\partial T}{\partial t} + V\cdot\nabla T - R$ (^{o}C/day) 11 August 1969, 1200Z, for the layer 850-200 mb. Shading denotes area covered by clouds on satellite photo.

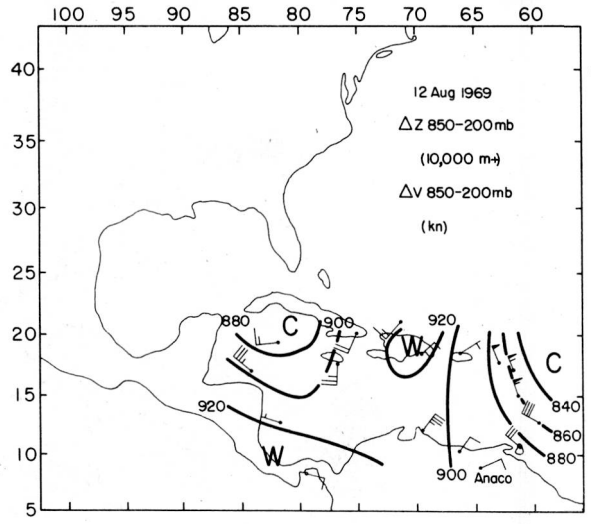

Figure 7. Wind shear vectors 850-200 mb (knots) and thickness between the 850 and 200-mb pressure surfaces (10,000 meters +) for 12 August 1969, 1200Z, illustrating relation between actual and geostrophic temperature fields.

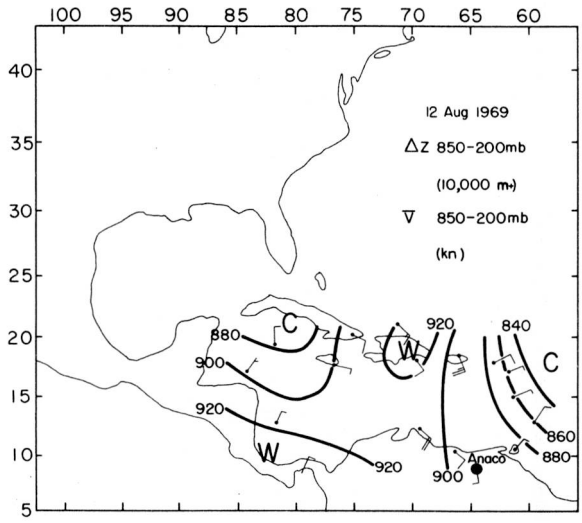

Figure 8. Thickness 850-200 mb for 12 August 1969 repeated from Fig. 4 and mean vector wind 850-200 mb (knots) showing regions of warm and cold advection.

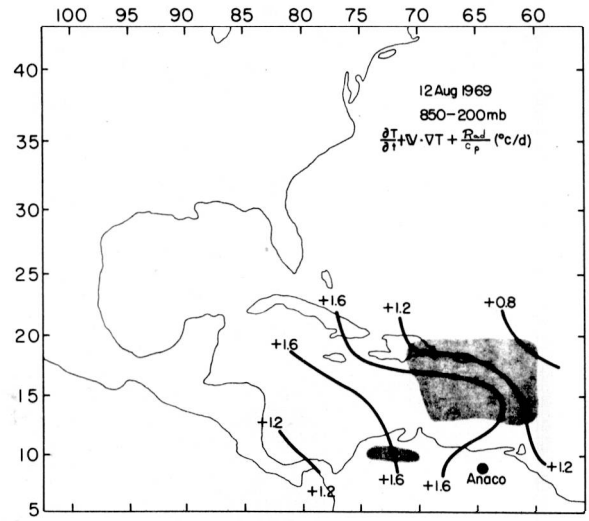

Figure 9. Field distribution of $\frac{\partial T}{\partial t} + V \cdot \nabla T - R$ (C^o/day) 12 August 1969, 1200Z, for the layer 850-200 mb. Shading denotes area covered by clouds on satellite photo.

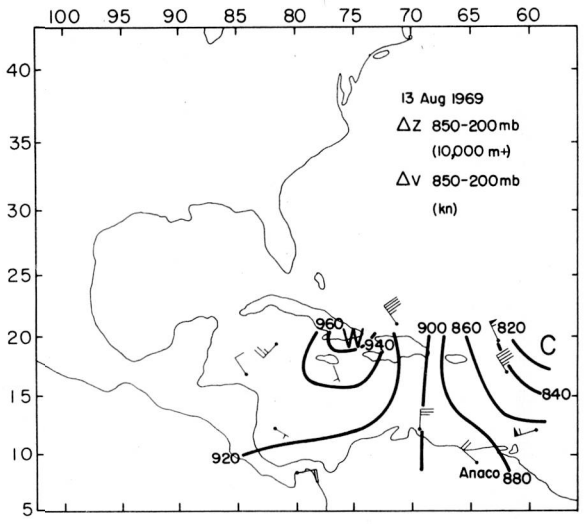

Figure 10. Wind shear vectors 850-200 mb (knots) and thickness between the 850 and 200-mb pressure surfaces (10,000 meters +) for 13 August 1969, 1200Z, illustrating relation between actual and geostrophic temperature fields.

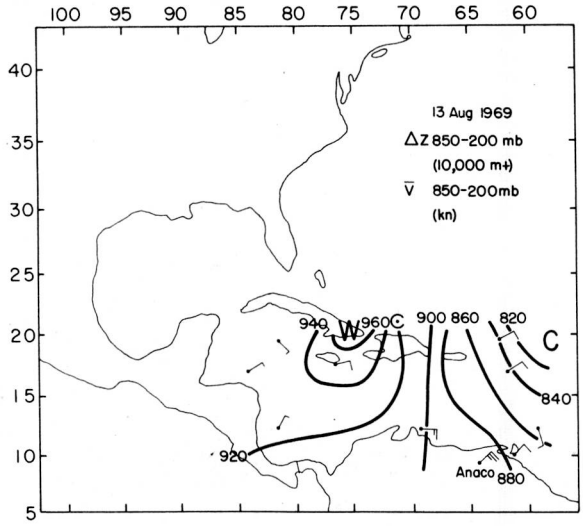

Figure 11. Thickness 850-200 mb for 13 August 1969 repeated from Fig. 4 and mean vector wind 850-200 mb (knots) showing regions of warm and cold advection.

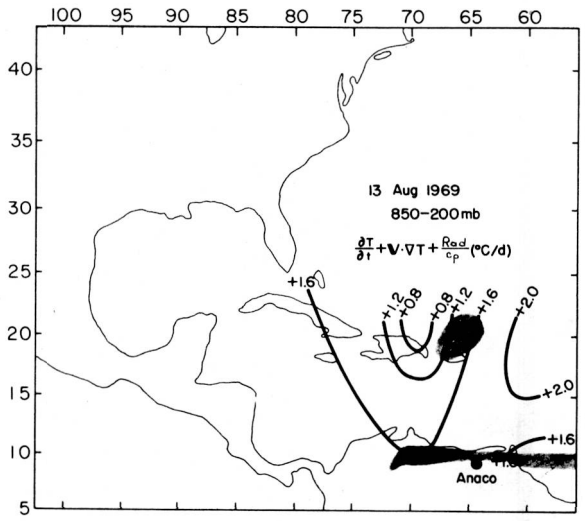

Figure 12. Field distribution of $\frac{\partial T}{\partial t} + V\cdot\nabla T - R$ (C^{o}/day) 13 August 1969, 1200Z, for the layer 850-200 mb. Shading denotes area covered by clouds on satellite photo.

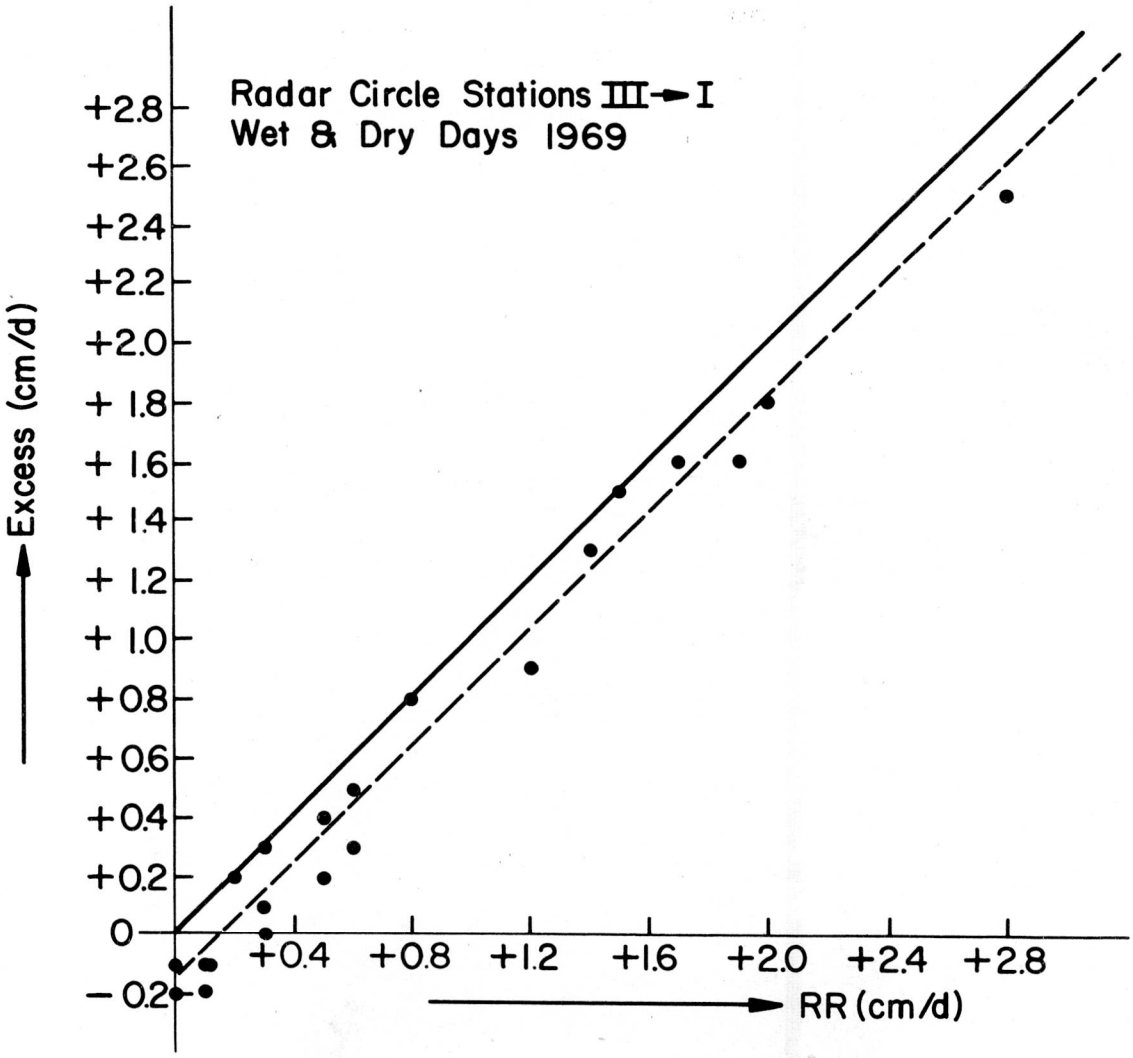

Figure 13. Correlation between P, P' and P'' for the radar circle on the analyzed days. The solid line gives perfect correlation; the area between solid and dashed lines indicates P' on the average, the area between dashed line and abscissa indicates P''.

RESULTS FOR THE ANACO AREA

Table II gives the results for the radar circle area around Anaco, where daily precipitation values were available. The dates appear on the left, in three-day sequences, and the corresponding synoptic types on the far right. The second column from the left gives the daily precipitation and the third column the corresponding classification of dry (d) or moist (m) for the day. Values of $(\frac{\partial T}{\partial t} + V \cdot \nabla T)$ and of radiation appear in the middle, expressed in terms of equivalent precipitation per day. Accordingly w is then given, either as area average downward on the left or as cloud ascent upward on the right. Excess precipitation and the ratio P''/P are also tabulated showing that on all days with large precipitation the ratio approaches 100 per cent. Figure 13 shows that the relation of P and P'' is very nearly linear. The area between solid and dashed lines represents the average P', the area between the dashed line and the abscissa represents P''. It is seen that a large fraction of the condensation heat liberated on the days chosen for analysis is exported and not locally retained in warming up the synoptic systems. It has been suggested that P'' represents hot tower precipitation, essentially a transformation from latent heat to potential energy without effect on vertical mass structure and horizontal gradients in the area of precipitation.

In Tables 12 and 13 the results are grouped for comparability between dry and moist sequences, and according to each day of the three-day sequences. Unfortunately, there are no differences beyond the obvious ones, especially in the importance of $\frac{\partial \hat{T}}{\partial t} + \widehat{V \cdot \nabla T}$ in relation

to precipitation, that would allow using the foregoing calculations as discriminant for synoptic analysis and forecasting.

It is of interest to compare the foregoing calculations with those of Betts (1972). Betts derived a model cloud from the VIMHEX project data with area of 500 km^2, duration of two hours and rain productiveness of 3.7 mm during that time or 18.5×10^2 cmx km^2. We can ask how many such model clouds are needed in order to yield our P' and P''; a similar question is considered by Riehl et al (1972). The radar circle area is 2×10^4 km^2; given a rainfall of 1 cm/day, we obtain water delivery of 200×10^2 cmx km^2/day. Division of the water yield of Betts' cloud gives $n = 10$ model clouds producing this radar circle precipitation. This is approximately equal to one cloud present continually and occupying 2.5 percent of the radar circle area.

Table 14 gives the total number of Betts' equivalent clouds for each day analyzed, also the number required for P' and P''. Clearly the number of such clouds producing the excess is preponderant; negative excess, from earlier considerations, indicates average descending motion. The conversion of Table 14 could serve as part of a means for parameterization of convective activity in the future.

TABLE 11

Table of Results

Date	RR (cm/day)	moist or dry	Dry (m/d) $\hat{w}\downarrow$	$\frac{\partial T}{\partial t} + V \cdot \nabla T$	Rad	Precipitation (cm/d) P''	%Excess Total	Cloud (m/d) $\hat{w}\uparrow$	Synoptic Class
7/9/69	0.5	m		0.1	0.2	0.2	40	120	III
7/10/69	1.5	m		-0.2	0.2	1.5	100	1000	III
7/11/69	1.7	m		-0.1	0.2	1.6	94	1080	I
8/7/69	0.1	d	-220	0.1	0.2	-0.2			III
8/8/69	2.0	m		0	0.2	1.8	90	1240	III
8/9/69	0	d	-360	0	0.2	-0.2			I
8/11/69	1.9	m		0.1	0.2	1.6	84	1080	III
8/12/69	2.8	m		0.1	0.2	2.5	90	1700	III
8/13/69	0.6	m		0.1	0.2	0.3	50	180	I
8/22/69	0.3	d		0.1	0.2	0		0	II
8/23/69	1.4	m		-0.1	0.2	1.3	93	880	III
8/24/69	0.8	m		-0.2	0.2	0.8	100	540	I
7/31/69	0.1	d	-110	0	0.2	-0.1			II
8/1/69	0.3	d		0	0.2	0.1	33	60	III
8/2/69	0.3	d		-0.2	0.2	0.3	100	180	I
8/19/69	0.5	m		-0.1	0.2	0.4	80	240	III
8/20/69	0.2	d		-0.2	0.2	0.2	100	120	III
8/21/69	0.1	d	-110	0	0.2	-0.1			I
9/8/69	1.2	m		0.1	0.2	0.9	75	620	III
9/9/69	0	d	-360	-0.1	0.2	-0.1			III
9/10/69	0.6	m		-0.1	0.2	0.5	83	300	I

TABLE 12

III → I Sequence Results for Wet Groups

1969	(D - 1)	(D)	(D + 1)
RR (cm/d)	0.5	1.5	1.7
	0.1	2.0	0
	1.9	2.8	0.6
	0.3	1.4	0.8
$\frac{\partial T}{\partial t} + V \cdot \nabla T$ (cm/d)	0.1	-0.2	-0.1
	0.1	0	0
	0.1	0.1	0.1
	0.1	-0.1	-0.2
	0.1		
Excess of RR (cm/d)	0.2	1.5	1.6
	-0.2	1.8	0.2
	1.6	2.5	0.3
	0	1.3	0.8
% $\frac{\text{Excess}}{\text{RR}}$	40	100	94
		90	
	84	90	50
		93	100
w↑ (clouds) (m/d)	+120	+1000	+1080
		+1240	
	+1080	+1700	+180
	0	+880	+540

TABLE 13

III → I Sequences Results for Dry Groups

1969	(D - 1)	(D)	(D + 1)
RR (cm/d)	0.1	0.3	0.3
	0.5	0.2	0.1
	1.2	0	0.6
$\frac{\partial T}{\partial t} + V \cdot \nabla T$ (cm/d)	0	0	-0.2
	-0.1	-0.2	0
	0.1	-0.1	-0.1
Excess of RR (cm/d)	-0.1	0.1	0.3
	0.4	0.2	-0.1
	0.9	-0.1	0.5
% $\frac{\text{Excess}}{\text{RR}}$		33	100
	80	100	
	75		83
w (m/d)	-110	+60	+180
	+240	+120	-110
	+620	-360	+300

TABLE 14

Comparison between Betts' Cloud Model and the Precipitation for the Area of Study

Date	RR (cm)	n (clouds)	n' (cloud)	n (Excess) (Clouds)
7/9/69	0.5	5	3	2
7/10/69	1.5	15	0	15
7/11/69	1.7	17	1	16
8/7/69	0.1	1	3	(-2)
8/8/69	2.0	20	2	18
8/9/69	0	0	2	(-2)
8/11/69	1.9	19	3	16
8/12/69	2.8	28	3	25
8/13/69	0.6	6	3	3
8/22/69	0.3	3	3	0
8/23/69	1.4	14	1	13
8/24/69	0.8	8	0	8
7/31/69	0.1	1	2	(-1)
8/1/69	0.3	3	2	1
8/2/69	0.3	3	0	3
8/19/69	0.5	5	1	4
8/20/69	0.2	2	0	2
8/21/69	0.1	1	2	(-1)
9/8/69	1.2	12	3	9
9/9/69	0	0	1	(-1)
9/10/69	0.6	6	1	5

RESULTS FOR OCEANIC AREA

Ascending motion in the cloudy areas and descending motion in the clear areas was calculated for the eastern Caribbean, also P' and the number of Betts' equivalent clouds for the cloudy areas. The latter, obtained from satellite photos, are shown shaded in the examples of Figs. 6, 9 and 12. Approximate areas of cloud cover were measured on each day. For the indicated values of $\frac{\partial T}{\partial t} + V \cdot \nabla T - R$, Table 9 gives the precipitation P' required for balance, while Table 10 gives the corresponding cloud vertical velocities. The number of Betts' equivalent clouds, of course, is determined by taking the size of oceanic area with cloud cover into account. Table 15 gives the results for all days.

9/10 Clear

CONCLUSION

Unfortunately, it has not been possible with kinematic, dynamic and heat balance calculations to find significant discriminants between dry and moist cases of synoptic systems and time evolution of such systems. Hopefully, however, enough progress in diagnostic approaches using synoptic charts has been realized that a renewed effort in the direction of the aims of this investigation will lead to a further advance during the conduct of VIMHEX II projected for the Venezuela rainy season of 1972.

REFERENCES

Bellamy, F. C., 1949: Objective calculations of divergence, vertical velocity and vorticity. Bulletin of the American Meteorological Society, Vol. 30, pp. 45-49.

Betts, A. K., 1972: A composite mesoscale cumulonimbus budget. Paper presented at the annual meeting of the AGU in Washington, D. C., April 17-21.

Rasmussen, J., 1969: Moisture analysis of an extratropical cyclone. Arch. Met. Geoph. Biokl., Ser. A, 18, 275-298.

Reed, R. J., 1971: Structure and properties of synoptic-scale wave disturbances in the equatorial western Pacific. Journal of Atmospheric Science, Vol. 28, No. 7, pp. 1117-1133, October.

Riehl, H., 1948: On the formation of west Atlantic hurricanes. Miscellaneous Report No. 24, Department of Meteorology, University of Chicago, pp. 1-67.

_____, and J. S. Malkus, 1958: On the heat balance in the equatorial trough zone. Geophysica, Vol. 6, 503-538.

_____, L. Cruz, M. Mata, and C. Muster, 1972: Precipitation characteristics during the Venezuelan rainy season. Paper presented at the annual meeting of the AGU in Washington, D. C., April 17-21.